View metadata, citation and similar papers at core.ac.uk
brought to you by CORE
provided by Elsevier - Publisher Connector

Cell, Vol. 115, 577–590, November 26, 2003, Copyright ©2003 by Cell Press

TSC2 Mediates Cellular Energy Response to Control Cell Growth and Survival

Ken Inoki,[1,2] Tianqing Zhu,[1,2] and Kun-Liang Guan[1,2,3,*]
[1]Life Sciences Institute
[2]Department of Biological Chemistry
[3]Institute of Gerontology
University of Michigan
Ann Arbor, Michigan 48109

Summary

Mutations in either the *TSC1* or *TSC2* tumor suppressor gene are responsible for Tuberous Sclerosis Complex. The gene products of TSC1 and TSC2 form a functional complex and inhibit the phosphorylation of S6K and 4EBP1, two key regulators of translation. Here, we describe that TSC2 is regulated by cellular energy levels and plays an essential role in the cellular energy response pathway. Under energy starvation conditions, the AMP-activated protein kinase (AMPK) phosphorylates TSC2 and enhances its activity. Phosphorylation of TSC2 by AMPK is required for translation regulation and cell size control in response to energy deprivation. Furthermore, TSC2 and its phosphorylation by AMPK protect cells from energy deprivation-induced apoptosis. These observations demonstrate a model where TSC2 functions as a key player in regulation of the common mTOR pathway of protein synthesis, cell growth, and viability in response to cellular energy levels.

Introduction

Tuberous sclerosis complex (TSC) is an autosomal dominant disorder caused by mutation in either the *TSC1* or *TSC2* tumor suppressor genes (Young and Povey, 1998). TSC is defined by the formation of hamartomas in a wide range of tissues. The TSC1 and TSC2 gene products are also known as hamartin and tuberin, respectively. They form a stable functional complex in vivo (van Slegtenhorst et al., 1998). Recent genetic studies in *Drosophila* demonstrate that the TSC1/TSC2 complex acts to negatively regulate cell growth and cell size (Gao and Pan, 2001; Ito and Rubin, 1999; Potter et al., 2001; Tapon et al., 2001). Homozygous mutation of *TSC1* or *TSC2* in mice is embryonic lethal due to cardiac hypertrophy and liver hypoplasia, while heterozygous mutation of either *TSC1* or *TSC2* significantly increases tumor incidence (Au et al., 1998; Kobayashi et al., 2001; Kwiatkowski, 2003; Onda et al., 1999). Studies in *Drosophila* have placed TSC1/TSC2 acting downstream of Akt in the insulin-signaling pathway and upstream of mammalian target of rapamycin (mTOR) (Gao and Pan, 2001; Gao et al., 2002; Potter et al., 2001; Tapon et al., 2001). Biochemical studies from several groups have demonstrated that TSC2 is a direct target of Akt (Dan et al., 2002; Inoki et al., 2002; Manning et al., 2002; Potter et al., 2002). Akt phosphorylation decreases the ability of TSC2 to inhibit the phosphorylation of ribosomal S6 kinase (S6K) and eukaryotic initiation factor 4E binding protein-1 (4EBP1), which are mTOR substrates. However, it has also been reported that TSC1/TSC2 may function to inhibit S6K independent of mTOR (Jaeschke et al., 2002; Radimerski et al., 2002).

Phosphorylation of S6K and 4EBP1 by mTOR play an important role in the regulation of translation (Brown et al., 1995; Hara et al., 1998; Shah et al., 2000). *TSC1* or *TSC2* mutant cells display elevated phosphorylation of both S6K and 4EBP1 (Goncharova et al., 2002; Kenerson et al., 2002; Kwiatkowski et al., 2002; Onda et al., 2002). In contrast, overexpression of TSC1 and TSC2 inhibits the phosphorylation of S6K and 4EBP1 (Goncharova et al., 2002; Inoki et al., 2002; Tee et al., 2002). Together, these results suggest that one of the major cellular functions of TSC1/TSC2 is to inhibit translation by inhibiting the phosphorylation of S6K and 4EBP1.

The rate of translation is regulated by multiple-signaling pathways including the availability of nutrients, growth factors, intracellular ATP levels, and environmental stress (Browne and Proud, 2002; Proud, 2002). ATP depletion decreases S6K and 4EBP1 phosphorylation and inhibits translation. It has been suggested that mTOR may sense cellular ATP levels because it has a high K_m (around 1 mM) for ATP (Dennis et al., 2001). However, this K_m value is still considerably lower than normal cellular ATP levels and therefore a drastic decrease in ATP would be required to affect the activity of mTOR (Proud, 2002). AMP is a much more sensitive indicator for cellular energy status, because cellular ATP concentration is much higher than AMP. A relatively small decrease in ATP levels will result in a relatively large increase in AMP levels that are sensed by and stimulate the 5′AMP-activated protein kinase (AMPK) (Hardie et al., 1998). Therefore, AMPK has been proposed as a physiological cellular energy sensor. 2-Deoxy glucose (2DG), a D-glucose analog, and 5-aminoimidazole-4-carboxyamide ribonucleotide (AICAR), activate AMPK (Corton et al., 1995) and increase phosphorylation of the eukaryotic elongation factor 2 (eEF2), indicating that AMPK plays a negative role in translation (Horman et al., 2002). It has been also reported that both 2DG and AICAR inhibit S6K activity (Kimura et al., 2003; Krause et al., 2002). The mechanism of S6K inhibition by AMPK appears to go through the mTOR pathway (Kimura et al., 2003). However, direct evidence of a molecular link between AMPK and mTOR remains to be determined.

In this report, we demonstrate that TSC2 is regulated by cellular energy levels. Activation of AMPK by energy starvation results in direct phosphorylation of TSC2 on T1227 and S1345. Knockdown of TSC2 protein by RNA interference eliminates the ATP depletion-induced dephosphorylation of S6K. In response to energy starvation, the $TSC2^{-/-}$ cells show a defective response in S6K dephosphorylation. Furthermore, the energy starvation-induced dephosphorylation of S6K is restored by the expression of wild-type TSC2, but not the AMPK phosphorylation mutant in $TSC2^{-/-}$ cells, demonstrating a

*Correspondence: kunliang@umich.edu

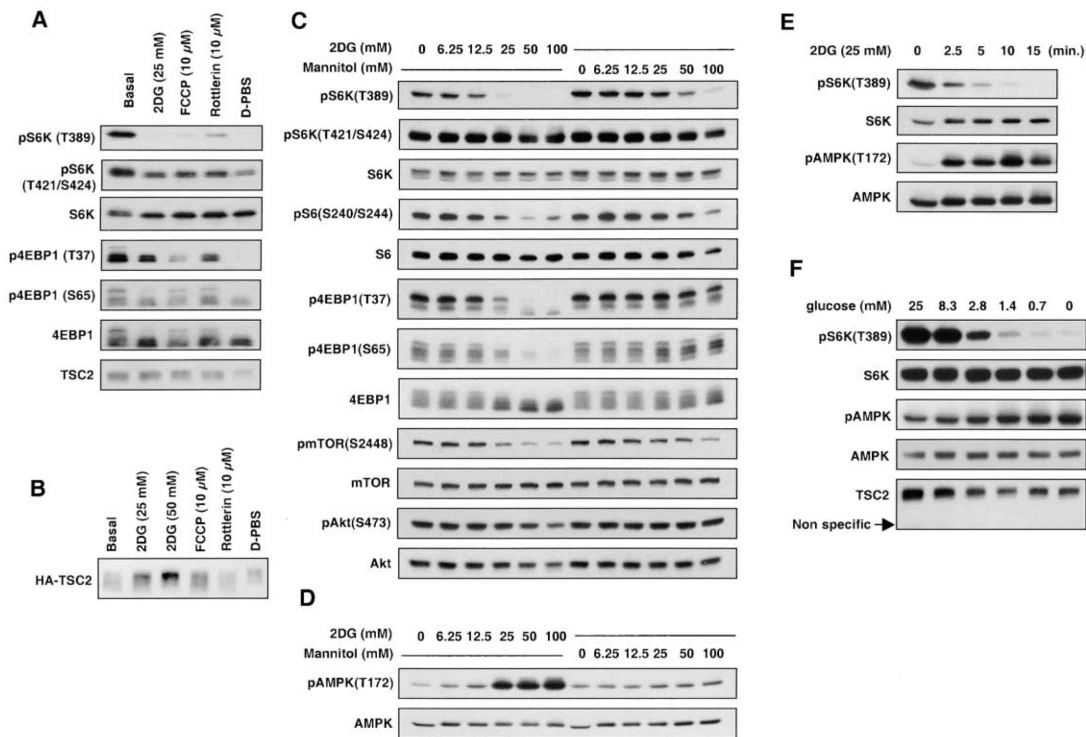

Figure 1. Effects of Energy Depletion on Phosphorylation of S6K, S6, 4EBP1, mTOR, Akt, AMPK, and TSC2

(A) Dephosphorylation of S6K and 4EBP1 by ATP depletion. HEK293 cells were treated with various agents as indicated for 15 min. Cell lysates were probed with indicated antibodies for phosphorylation of endogenous proteins.

(B) Mobility shift of TSC2. HEK293 cells were transfected with HA-TSC2 and TSC1. Lysates were resolved by a 5% SDS-PAGE gel and probed with anti-HA.

(C) 2DG-induces dephosphorylation of endogenous S6K, S6, 4EBP1, mTOR, but not Akt. HEK293 cells were treated with the indicated concentration of 2DG or mannitol for 15 min. Phosphorylation of endogenous proteins were determined by Western blotting using specific antibodies or phosphospecific antibodies as indicated on the left of each strip.

(D) 2DG-induces phosphorylation of AMPK.

(E) Time course of 2DG treatment.

(F) Low glucose inhibits S6K. HEK293 cells were cultured in media with indicated concentrations of glucose for 2 hr. All Western blots were performed with endogenous proteins.

critical function of TSC2 phosphorylation by AMPK in the regulation of translation by cellular energy starvation. TSC2 plays an essential role to control cell size in response to energy limitation and to protect cells from glucose deprivation-induced apoptosis. Moreover, AMPK-dependent phosphorylation of TSC2 is important for TSC2 function in cell size regulation and cell survival under energy starvation conditions. Our studies demonstrate an essential role of TSC2 and AMPK phosphorylation in the cellular energy response.

Results

ATP Depletion Induces TSC2 Phosphorylation

Protein synthesis is regulated by multiple cellular conditions including cellular energy levels. We observed that depletion of cellular ATP by the glucose analog 2-deoxyglucose (2DG, which blocks cellular glucose utilization by indirectly inhibiting hexokinase), mitochondrial uncoupler FCCP, and the PKC inhibitor Rottlerin (Soltoff, 2001) caused a dephosphorylation of S6K and 4EBP1 (Figure 1A). In addition, depletion of nutrients by culturing cells in D-PBS inhibited the phosphorylation of S6K and 4EBP1 (Hara et al., 1998). Interestingly, ATP depletion and nutrients deprivation also resulted in a significant mobility upshift of TSC2 (Figure 1B), indicating that TSC2 phosphorylation is possibly enhanced by these cellular conditions.

Dennis et al. (2001) have previously reported that 2DG treatment using concentrations between 20 and 100 mM achieved 50 to 70% reduction of intracellular ATP levels and resulted in inhibition of S6K and 4EBP1 phosphorylation. They concluded that the inhibition of S6K and 4EBP1 phosphorylation by 2DG is directly due to the sensing of lowered ATP levels by mTOR, which has a K_m for ATP of around 1 mM (Dennis et al., 2001). We observed that mannitol, an osmolite, at 100 mM also significantly inhibited the phosphorylation of S6K (Figure 1C), suggesting that the effect of high concentration of 2DG could be due to a mixed response of depletion of cellular ATP level and its acting as an osmolite. We observed that at low concentrations of 2DG, such as 25 mM, phosphorylation of S6K on T389 was effectively inhibited while a similar concentration of mannitol had little effect (Figure 1C). Similar observations were observed with the phosphorylation of S6 and 4EBP1 (Fig-

ure 1C). Phosphorylation of mTOR S2448, which may correlate with mTOR activity (Nave et al., 1999; Scott et al., 1998; Sekulic et al., 2000), was also inhibited by 25 mM 2DG (Figure 1C). In contrast, 25 mM 2DG had little effect on Akt phosphorylation. These results demonstrate that 2DG specifically inhibits the phosphorylation of S6K, 4EBP1, and mTOR but does not signal through Akt.

AMPK is much more sensitive to changes in cellular energy status than mTOR because it is activated by the ratio of AMP/ATP. 25 mM 2DG-activated AMPK as indicated by the dramatic increase of T172 phosphorylation in AMPK (Figure 1D) (Hardie and Hawley, 2001). 2DG at 25 mM induced rapid AMPK activation and concomitant dephosphorylation of S6K as a function of treatment time (Figure 1E). Our observations are consistent with recent reports that AMPK activation closely correlates with the inhibition on S6K and 4EBP1 (Horman et al., 2002; Kimura et al., 2003; Krause et al., 2002). These data suggest that activation of AMPK may be responsible for the ATP-depletion induced dephosphorylation of S6K and 4EBP1. We observed a statistically significant reduction of ATP levels and an increase of AMP/ATP ratio in cells treated with 25 mM 2DG (Supplemental Figures S1A and S1B available at http://www.cell.com/cgi/content/full/115/5/577/DC1). However, based on previously published data, such a decrease in ATP concentration would not significantly affect mTOR kinase activity (Dennis et al., 2001). This suggests that AMPK is the prime energy sensor in response to mild energy depletion. Glucose limitation also decreased S6K phosphorylation, increased AMPK phosphorylation, and caused a mobility shift of TSC2 (Figure 1F).

2DG Stimulates the Interaction between Endogenous AMPK and TSC2

The fact that 2DG induces AMPK activation and a mobility upshift of TSC2 suggests that AMPK may be responsible for TSC2 phosphorylation. We first examined whether AMPK and TSC2 interact. Immunoprecipitation of AMPK indicated that both TSC1 and TSC2 are weakly coimmunoprecipitated by AMPK (Figure 2A). TSC2 and TSC1 were found to interact preferentially with AMPK following 2DG stimulation. We also performed coimmunoprecipitations with the anti-phospho AMPK antibody (pAMPK), which recognizes the active form of AMPK. Interestingly, this antibody specifically precipitated the active, hence slower, migrating form of AMPK from both control and 2DG-treated cell lysates (Figure 2A). However, no TSC2 or TSC1 was recovered in the anti-pAMPK immunoprecipitates. This observation is not surprising because T172 in AMPK is localized in the activation loop (Scott et al., 2002; Stein et al., 2000). Binding of antibody to this site may block substrate binding based on known kinase structures.

To determine whether active AMPK is associated with TSC2, we performed reciprocal coimmunoprecipitation with anti-TSC2 antibody followed by Western blotting with anti-AMPK and anti-pAMPK antibody. The interaction between endogenous AMPK and TSC2 was enhanced by 2DG (Figure 2B). Figure 2C shows that the levels of proteins in the lysates are similar. The above observations demonstrate that 2DG treatment stimulates the interaction between endogenous TSC2 and AMPK.

We also performed coimmunoprecipitation studies between endogenous AMPK and overexpressed TSC2 and confirmed that 2DG enhances the interaction between TSC2 and AMPK (Figure 2D). Deletion analysis showed that the C-terminal domain of TSC2 is responsible for the interaction with AMPK while the N-terminal domain is not required.

TSC2 Is Required to Mediate the Cellular Energy Response

To determine the role of TSC2 in S6K inactivation by 2DG, HEK293 cells were treated with TSC2 RNAi oligos. TSC2 RNAi significantly decreased endogenous TSC2 protein levels, but had no effect on the unrelated protein MEK2 (Figure 3A). 2DG-induced S6K dephosphorylation was blocked in TSC2 knockdown cells, but not in the control cells. In contrast, knockdown of TSC2 had no significant effect on AMPK phosphorylation in response to 2DG. Inhibition of mTOR by rapamycin-blocked S6K phosphorylation even when TSC2 expression was knocked down suggesting that mTOR is downstream of TSC2 (Figure 3B).

We further examined the function of AMPK in S6K regulation. Coexpression of the active AMPK αI or αII catalytic subunit resulted in a decrease of S6K phosphorylation (Figure 3C), supporting that AMPK negatively controls S6K phosphorylation. Knockdown of TSC2 by RNAi blocked the inhibitory effect of AMPK expression, suggesting that TSC2 acts downstream of AMPK. Neither TSC2 RNAi nor rapamycin significantly affected the phosphorylation of acetyl CoA carboxylase (ACC) and eukaryote elongation factor 2 (eEF2), two AMPK substrates (Supplemental Figures S2A and S2B available on *Cell* website), supporting the specific role of TSC2 in mediating AMPK on S6K regulation.

If TSC2 plays a role in mediating S6K inhibition by ATP depletion, EEF8 (TSC2$^{-/-}$) and the EEF4 (TSC2$^{+/+}$) fibroblasts should respond differently to various ATP depletion reagents. As expected, EEF8 cells show a much higher level of S6K phosphorylation (Figure 3D). In order to compare the results of EEF4 and EEF8 cells, both long and short exposures of the S6K phosphorylation immunoblot are presented in Figure 3D. We observed that Rottlerin, FCCP, and to a lesser extent, azide, oligomycin, and rotenone caused a decrease in S6K phosphorylation in EEF4 cells. The effects of these reagents on S6K phosphorylation are much weaker in EEF8 cells (Figure 3D). Similar results were observed with the phosphorylation of 4EBP1. However, the activation of AMPK was not different between the EEF4 and the EEF8 cells (Figure 3D). These data further support the notion that TSC2 plays an important role in mediating the effect of ATP depletion on the phosphorylation of S6K and 4EBP1. We performed similar experiments with 2DG and D-PBS treatment. In EEF8 (TSC2$^{-/-}$) cells, 2DG and D-PBS had little effect on 4EBP1 phosphorylation. This is in contrast to the inhibition of phosphorylation of 4EBP1 in the EEF4 (TSC2$^{+/+}$) cells (Figure 3E). Our data are consistent with previously published observations that nutrient depletion-induced S6K dephosphorylation is compromised in TSC2$^{-/-}$ cells (Gao et al., 2002).

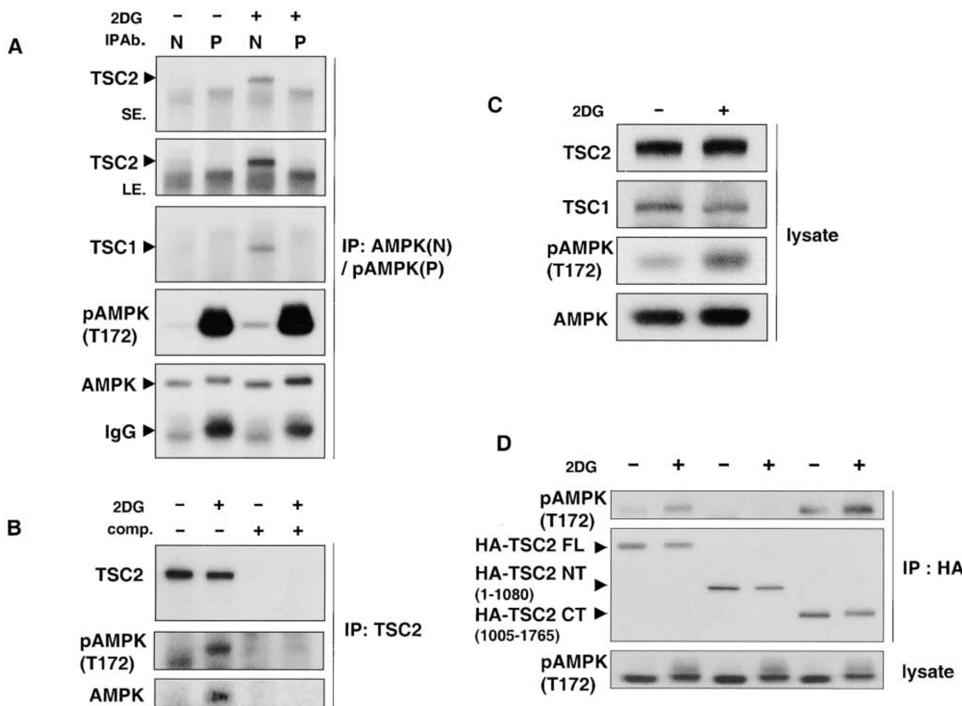

Figure 2. ATP Depletion Stimulates the Interaction of Endogenous AMPK and TSC2

(A) 2DG stimulates the coimmunoprecipitation between endogenous TSC2 and AMPK. HEK293 cells were treated with 25 mM 2DG for 2.5 min. Cell lysates were immunoprecipitated with anti-AMPK (N) or anti-phospho AMPK (P) antibody. The immunoprecipitates were blotted with indicated antibodies for TSC2, TSC1, pAMPK, and AMPK. IP denotes immunoprecipitation. SE. and LE. denote short exposure and long exposure, respectively.

(B) Reciprocal immunoprecipitation of endogenous TSC2 and AMPK. Cell lysates were subject to immunoprecipitation with anti-TSC2 antibody. Preincubation of anti-TSC2 antibody with TSC2 peptide (Santa Cruz) was included as a control for the competition (comp).

(C) Expression levels of endogenous TSC1, TSC2, pAMPK, and AMPK in lysates of HEK293 cells.

(D) The C-terminal fragment of TSC2 interacts with endogenous AMPK. HEK293 cells were transfected with HA-TSC2 WT, HA-TSC2 N-terminal (1–1080) and HA-TSC2 C-terminal (1005–1765). The cell lysates were immunoprecipitated with HA antibody followed by Western blot with anti-HA or anti-pAMPK.

TSC2 Is Phosphorylated by AMPK

Treatment with lambda phosphatase converted TSC2 to a faster migrating band (Figure 4A), which suggests that the 2DG-induced mobility shift is due to phosphorylation. TSC1 is also a phosphoprotein, which is downshifted by lambda phosphatase treatment (Figure 4A). However, 2DG treatment did not alter the mobility of TSC1. Cotransfection of active AMPK αI also induced a mobility upshift of TSC2, but not of TSC1, suggesting that AMPK regulates TSC2 phosphorylation (Figure 4B). Incubation of HEK293 cells with 10 μM AMPK inhibitor (Zhou et al., 2001) increased the mobility of TSC2, supporting a role for endogenous AMPK in TSC2 phosphorylation (Figure 4C).

The functional relationship between AMPK and 2DG-induced S6K dephosphorylation was examined by expressing dominant-negative AMPK. Dose-dependent expression of the kinase inactive catalytic subunit αII of AMPK (AMPK-DN) partially blocked S6K inhibition by 2DG treatment (Figure 4D). Furthermore, incubation of HEK 293 cells with an AMPK inhibitor significantly reversed the inhibitory effect of 2DG on S6K phosphorylation (Figure 4E). AMPK inhibitor also significantly blocked S6K dephosphorylation induced by glucose deprivation (Figure 4F). Together, these data strongly support our hypothesis that AMPK activation plays an important role in TSC2 phosphorylation and S6K inhibition in response to energy starvation.

T1227 and S1345 in TSC2 Are Major AMPK Phosphorylation Sites

To elucidate the mechanism of TSC2 regulation by AMPK, we performed in vivo labeling and two-dimensional phosphopeptide mapping of TSC2. Stimulation with 2DG (25 and 40 mM) enhanced phosphorylation of several peptides (Figure 5A, a–c). Interestingly, coexpression of the active AMPK αI subunit also increased phosphorylation of the same peptides stimulated by 2DG (Figure 5A, a and d). The shaded spots in Figure 5A, image e denote phosphopeptides induced by 2DG or AMPK. These results clearly demonstrate that AMPK plays a major role in TSC2 phosphorylation induced by 2DG.

We searched the TSC2 sequence for AMPK recognition consensus sites (Hardie et al., 1998) and found that rat TSC2 contains 8 putative AMPK sites (Supplemental Figure S3 available on *Cell* website). We mutated all putative AMPK sites individually and performed two-dimensional phosphopeptide mapping. Our data indicate that all the individual mutants, except for T1227A

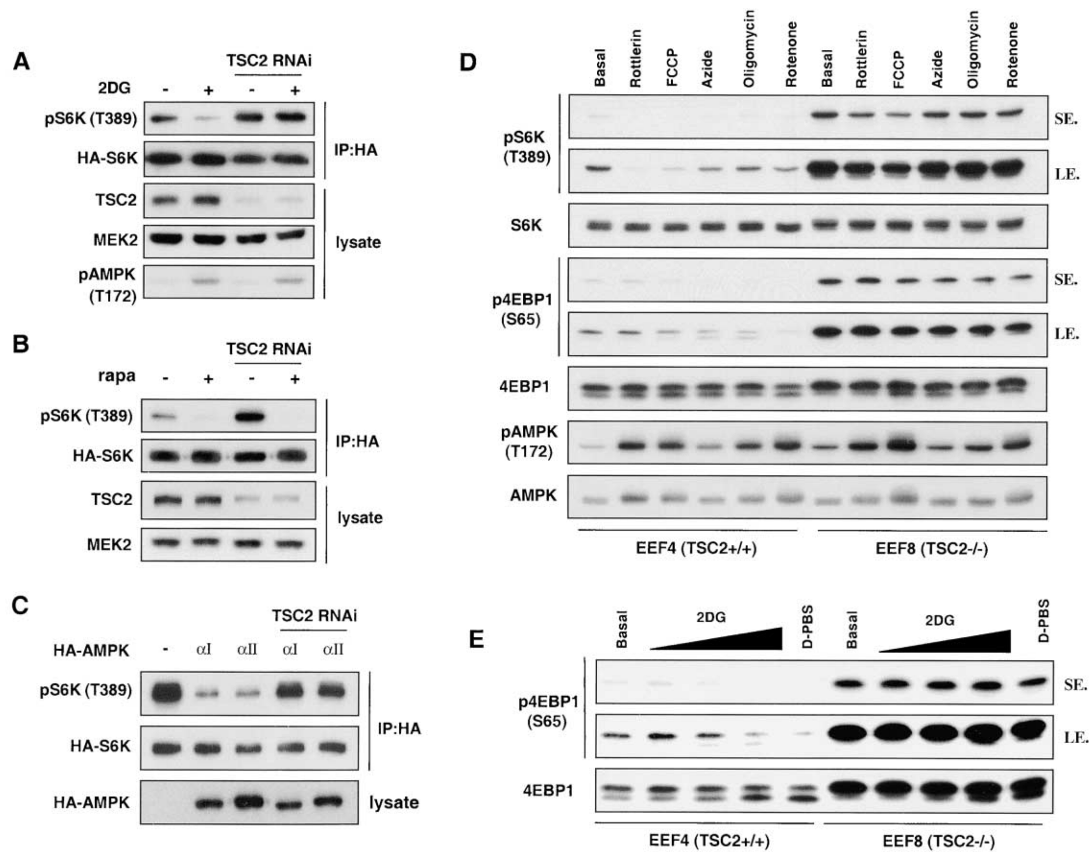

Figure 3. TSC2 Is Required for ATP Depletion-Induced Dephosphorylation of S6K

(A) Knockdown of TSC2 by RNA interference blocks the 2DG response. HEK293 cells were cotransfected HA-S6K and TSC2 RNAi as indicated. Cells were stimulated with 2DG for 15 min. HA-S6K was immunoprecipitated with anti-HA antibody and Western blotted with anti-phospho S6K(T389) and anti-HA.

(B) Knockdown of TSC2 by RNA interference does not block rapamycin-induced dephosphorylation of S6K. Experiments were similar to Figure 3A, except rapamycin (20 nM for 30 min preincubation) was used to treat the HEK293 cells.

(C) Inhibition of S6K by AMPK overexpression is blocked by TSC2 RNAi. HA-S6K was cotransfected with the active AMPK αI or αII subunit as indicated. Cotransfection of TSC2 RNAi is indicated. HA-S6K was immunoprecipitated and phosphorylation of S6K was determined. The expression of transfected HA-AMPK was also determined by Western blotting.

(D) ATP depletion-induced dephosphorylation of S6K and 4EBP1 are compromised in $TSC2^{-/-}$ cells. EEF4 ($TSC2^{+/+}$) and EEF8 ($TSC2^{-/-}$) cells were treated with various reagents for 15 min (rottlerin 10 μM, FCCP 10 μM, azide 1 mM, oligomycin 6.3 μM, and rotenone 20 μM). Phosphorylation of endogenous S6K, 4EBP1, and AMPK was determined. Two different exposures (SE. short exposure, LE. long exposure) of pS6K (T389) and p4EBP1(S65) are presented.

(E) 2DG-induced 4EBP1 dephosphorylation is compromised in $TSC2^{-/-}$ cells. EEF4 and EEF8 cells were treated with 2DG (12.5 mM, 25 mM, and 50 mM) in DMEM/F12 medium or D-PBS for 30 min. Phosphorylation of 4EBP1 was determined.

and S1345A, had phosphopeptide maps similar to the wild-type TSC2 (data not shown). Interestingly, the S1345A mutant affected the majority of the 2DG and AMPK inducible phosphopeptides (spots 1–3, 5–8 in image f, Figure 5A). These results support the hypothesis that S1345 is likely an AMPK phosphorylation site in vivo. Furthermore, phosphorylation of S1345 may affect phosphorylation of other residues, such as S1337 and S1341, which are adjacent to the AMPK, site S1345 (Figure 5B).

To confirm whether S1345 can be phosphorylated by AMPK directly in vitro, a TSC2 fragment containing S1345 was expressed and purified (Figure 5C). The TSC2 fragment was phosphorylated by immunoprecipitated AMPK, but not the kinase inactive AMPK mutant (Figure 5C, top image). Mutation of S1345 to either alanine (S1345A) or aspartate (S1345D) completely eliminated the in vitro phosphorylation of TSC2 by AMPK, indicating that S1345 is a direct AMPK phosphorylation site. These data also suggest that S1337 and S1341 are not direct AMPK phosphorylation sites (Figure 5C) although phosphorylation of these residues is enhanced by 2DG and AMPK in vivo (Figures 5A and 5B). Mixing of in vitro phosphorylated TSC2 fragment with the in vivo phosphorylated TSC2-S1345A mutant demonstrate that the in vitro AMPK phosphorylation sites in TSC2 are indeed phosphorylated in vivo (Figure 5D). We also observed that T1227 is phosphorylated by AMPK (Supplemental Figure S4 available on *Cell* website).

Mutation of S1345 affected multiple phosphorylation sites including S1337 and 1341 even though these are not AMPK consensus (Figures 5A and 5B). We created the TSC2-S1337/1341/1345A (TSC2-3A) triple mutant and tested the mobility shift induced by 2DG. The 2DG

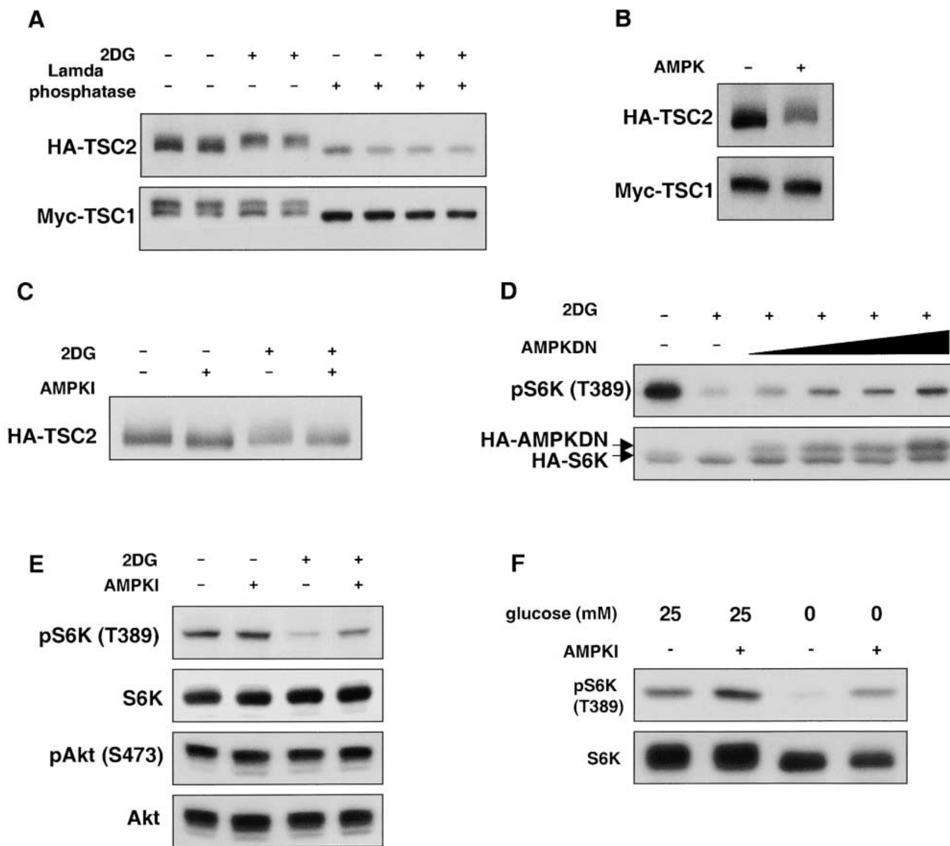

Figure 4. ATP Depletion and AMPK Induce TSC2 Phosphorylation

(A) 2DG-induced TSC2 mobility shift is due to phosphorylation. HA-TSC2 and Myc-TSC1 were transfected into HEK293 cells and treated with 25 mM 2DG for 15 min as indicated. Cell lysates were treated with lambda phosphatase to determine phosphorylation state.

(B) Active AMPK αI expression induces a slow migrating form of TSC2.

(C) An AMPK inhibitor blocks the 2DG induced mobility shift of TSC2. AMPK inhibitor (Compound C, 10 μM) was added 30 min before the treatment of 2DG as indicated.

(D) Kinase inactive AMPK mutant blocks 2DG-induced dephosphorylation of S6K. HEK293 cells were transfected with increasing amounts of the kinase inactive AMPK mutant (AMPKDN). Phosphorylation of cotransfected HA-S6K was determined.

(E) AMPK inhibitor blocks the 2DG-induced dephosphorylation of S6K. HEK293 cells were treated with AMPKI (10 μM) for 30 min prior to the addition of 2DG. Phosphorylation of endogenous S6K and Akt was determined.

(F) AMPK inhibitor partially blocks S6K dephosphorylation induced by glucose deprivation. HEK293 cells were cultured in media with indicated concentration of glucose for 2 hr in the presence or absence of AMPK inhibitor (10 μM).

dependent upshift was largely abolished in the triple mutant (Figure 5E), indicating that these residues are major phosphorylation sites induced by energy starvation.

AMPK Phosphorylation Enhances TSC2 Function

The functional significance of AMPK phosphorylation was assessed by using TSC2 phosphorylation mutants. HEK 293 cells transfected with TSC2-3A mutant showed that this mutant was less able to inhibit S6K in response to 2DG treatment (Figure 6A). This result is consistent with the notion that phosphorylation by AMPK promotes the ability of TSC2 to inhibit S6K. We also tested the ability of TSC2-3A to interact with TSC1 and found that the mutant TSC2 was able to form a complex with TSC1 normally (Figure 6B).

To examine whether phosphorylation of TSC2 by AMPK plays a role in the dephosphorylation of S6K and 4EBP1 in response to 2DG treatment, we transiently infected EEF8 ($TSC2^{-/-}$) fibroblast cells with a retrovirus expressing either the wild-type or the T1227A/S1345A mutant. As expected, expression of TSC2 reduced the basal phosphorylation of S6K and 4EBP1 (Figure 6C). Treatment with 2DG caused little decrease of S6K and 4EBP1 phosphorylation in the vector-infected cells. In contrast, 2DG significantly decreased S6K and 4EBP1 phosphorylation in wild-type TSC2-expressing cells (Figure 6C). Interestingly, cells expressing the TSC2–T1227A/S1345A mutant were less responsive to 2DG treatment than those expressing wild-type TSC2 (Figure 6C). These data support a model that the AMPK-dependent phosphorylation of T1227 and S1345 in TSC2 plays an important role in the cellular response to 2DG treatment.

To further establish the functional importance of TSC2 and AMPK phosphorylation in response to changes in the cellular energy, we established stable TSC2-expressing cell lines from the $TSC2^{-/-}$ LEF cells that are derived

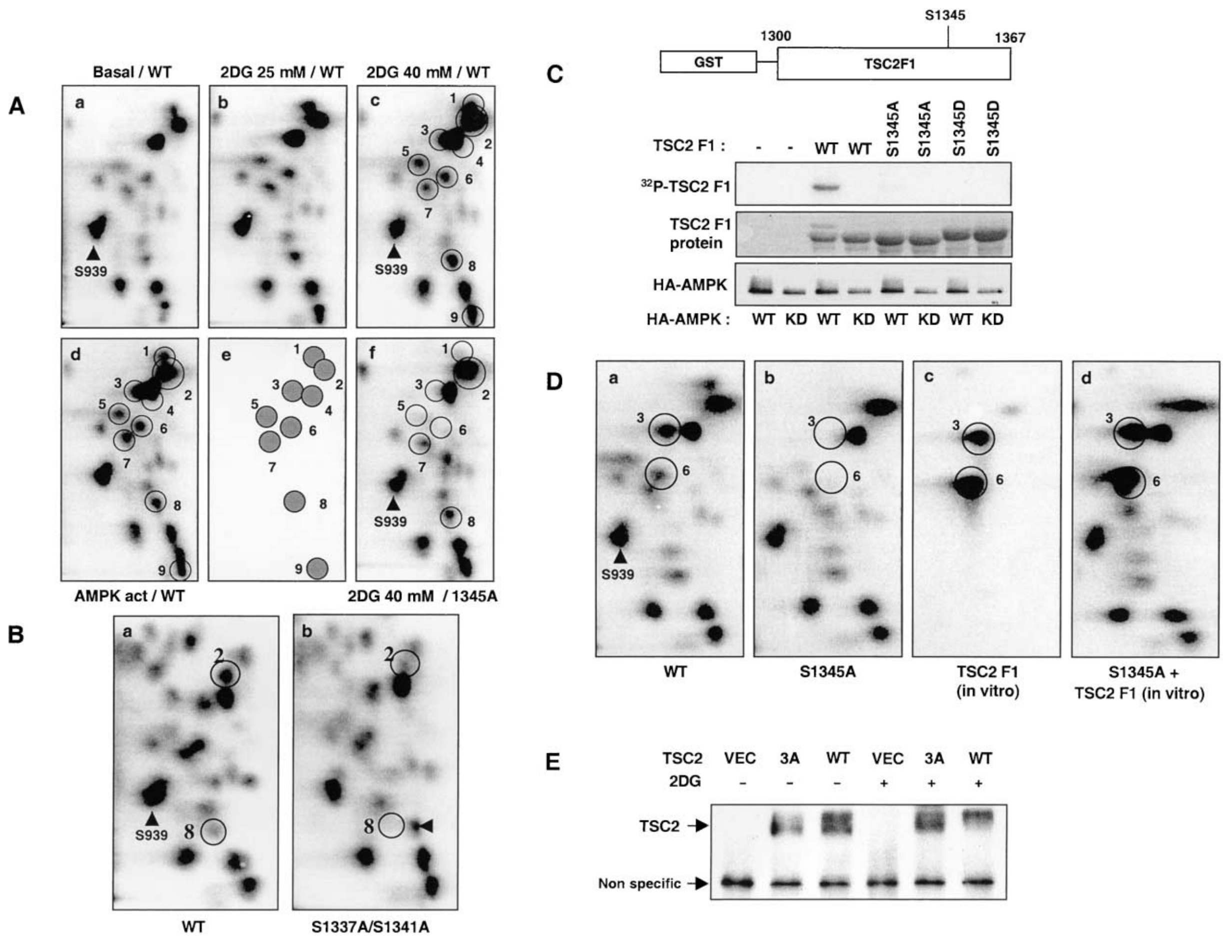

Figure 5. AMPK Phosphorylates TSC2 on S1345

(A) 2DG and AMPK induce TSC2 phosphorylation on multiple spots in vivo. HA-TSC2 was cotransfected with TSC1 in HEK 293 cells. Cells were labeled with ^{32}P-phosphate. HA-TSC2 was analyzed by a two-dimensional phosphopeptide mapping. Phosphopeptides of basal (a), treatment with 2DG (b and c), active AMPK αI subunit cotransfection (d), and the TSC2-S1345A mutant with 2DG treatment (f) are indicated. Image e is a schematic representation of phosphopeptides. The shaded spots denote those that are increased by 2DG treatment or AMPK cotransfection. The arrowhead indicating S939 (Akt phosphorylation spot) is used as a reference marker.

(B) S1337 and S1341 are AMPK-dependent sites phosphorylated by 2DG treatment. Two-dimensional phosphopeptide mapping of wild-type and TSC2-A1337A/S1341A mutant. Spot 2 and 8 are missing in the mutant. Furthermore, a new spot appears in the mutant as indicated by an arrowhead.

(C) AMPK directly phosphorylates TSC2 on S1345 but not S1337 or 1341 in vitro. The TSC2 fragment (residues 1300–1367) was expressed as a GST fusion (GST-TSC2 F1) and purified from *E. coli*. Wild-type AMPK αI (WT) or the kinase inactive AMPK αI (KD) plasmids were transfected into HEK293 cells and immunoprecipitated. GST-TSC F1 was phosphorylated in vitro by immunoprecipitated AMPK and detected by autoradiography (top image). Coomassie blue staining of the recombinant TSC2 F1 is shown in the middle image. The amount of AMPK used in the kinase assay is shown in the bottom image. S1345A and S1345D denote mutations of Ser1345 in TSC2 F1 replaced by alanine and aspartate, respectively.

(D) Ser1345 in TSC2 is phosphorylated in vivo. Two-dimensional phosphopeptide mapping of in vivo label and in vitro phosphorylated TSC2. Mutation of S1345 resulted in elimination of multiple phosphopeptide spots, including spots 3 and 6 (a and b). Image c is the 2-D map of the in vitro phosphorylated TSC2 by AMPK. Image d, 2-D map of the mixture of in vivo labeled TSC2-S1345A and the in vitro phosphorylated TSC2 F1.

(E) Wild-type TSC2 but not the S1337A/S1341A/S1345A (3A) mutant shows a mobility shift in response to 2DG. EEF8 ($TSC2^{-/-}$) cells were infected with retrovirus encoding the TSC2 or TSC2-3A, and treated with 2DG as indicated.

from an epithelial origin. Expression of TSC2 decreased S6K phosphorylation while expression of the TSC2-3A had a much weaker effect on S6K (Figure 6D). Importantly, glucose deprivation decreased in S6K phosphorylation in the wild-type TSC2-expressing cells, but had a much smaller effect in the vector or the TSC2-3A-expressing cells even though AMPK activation was unaffected (Figure 6E). These results clearly demonstrated that TSC2 is required for S6K inactivation by glucose deprivation. Furthermore, phosphorylation of TSC2 by AMPK is required for the cellular response to energy limitation.

TSC Protects Cells from Glucose Deprivation-Induced Apoptosis

To determine the physiological relevance of TSC2 in energy sensing pathway, we examined the effect of energy starvation on cell viability. We found that the vector-

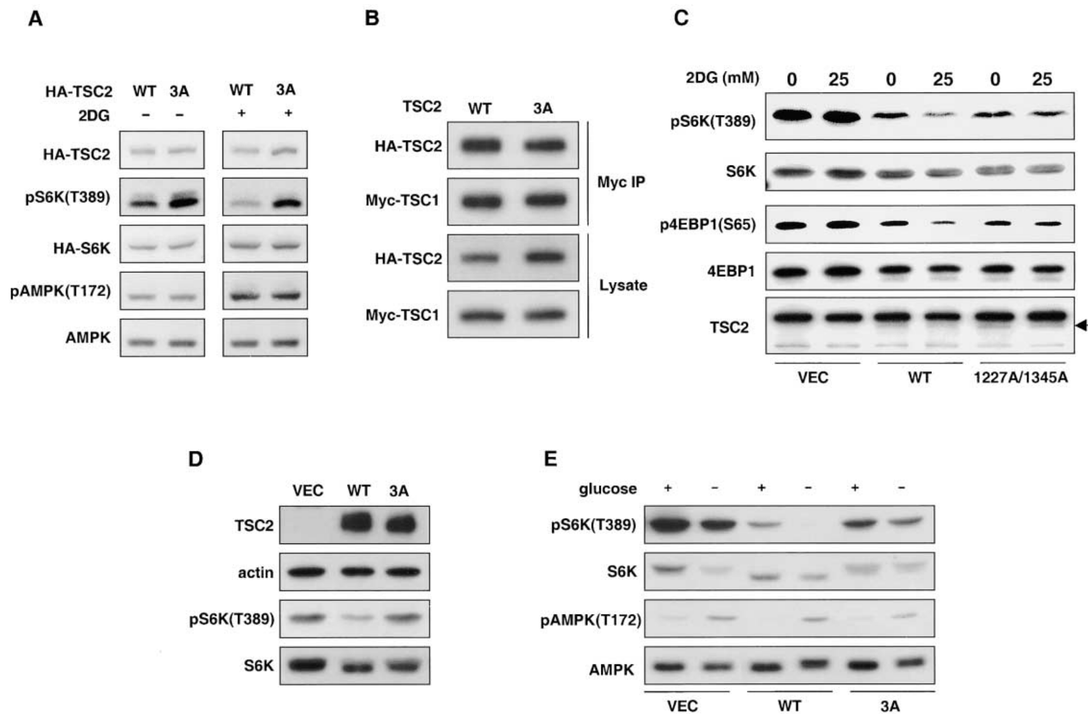

Figure 6. AMPK Phosphorylation Is Important for TSC2 Function in the Regulation of S6K Phosphorylation in Response to Energy Starvation

(A) Mutation of the AMPK-dependent sites in TSC2 decreases TSC2 activity. HEK293 cells were transfected with wild-type or mutant TSC2 as indicated. The anti-pS6K(T389) blot was exposed for longer time in the right image.

(B) Mutant TSC2 can form complex with TSC1.

(C) Cells expressing the AMPK phosphorylation mutant TSC2 (T1227A/S1345A) are less responsive to 2DG treatment. The EEF8 (TSC2$^{-/-}$ fibroblast) cells were transiently infected with wild-type or mutant TSC2 retrovirus as indicated. Phosphorylation of endogenous S6K and 4EBP1 was determined. The arrow indicates the expression of wild-type and mutant TSC2, which just below the nonspecific band detected by anti-TSC2.

(D) TSC2-3A mutant is less active to inhibit S6K. LEF (TSC2$^{-/-}$ epithelial) cells were infected with TSC2 retrovirus and selected for the neomycin-resistant stable-expressing cells. Expression of TSC2 was determined by immunoprecipitation and Western blot with anti-TSC2 antibody. Phosphorylation of endogenous S6K was determined.

(E) The AMPK-dependent phosphorylation of TSC2 is important for glucose deprivation-induced S6K dephosphorylation. Stable LEF cells infected with vector, TSC2, and TSC2-3A were cultured in the presence (25 mM) or absence of glucose for 16 hr. Phosphorylation of endogenous S6K and AMPK was determined.

infected LEF cells underwent massive cell death 72 hr after shifting to glucose-free conditions (Figure 7A). In contrast, the TSC2-expressing LEF cells showed little increase in cell death, suggesting that TSC2 rescued cell death by glucose starvation (Figure 7A). To determine the significance of AMPK phosphorylation in TSC2 function, we also examined the TSC2-3A-expressing LEF cells. Interestingly, TSC2-3A failed to protect LEF cells from glucose deprivation-induced cell death (Figure 7A). Furthermore, rapamycin treatment almost completely suppressed glucose deprivation-induced cell death in LEF (Vec) and LEF (3A) cells (Figure 7A). These data suggest that the uncontrolled high mTOR activity is responsible for cell death under energy starvation conditions.

We performed experiments to examine whether glucose deprivation induces apoptosis. A fluorescence-based assay for DNA fragmentation showed that glucose deprivation induced apoptosis in vector and TSC2-3A, but not in TSC2-expressing LEF cells (Figure 7B). Western blots for apoptosis markers revealed that both caspase 3 and PARP were cleaved during glucose deprivation (Figure 7C). Rapamycin treatment suppressed caspase 3 activation in the TSC2$^{-/-}$ and TSC2-3A-expressing cells (Figure 7D). We also tested the effect of energy deprivation in the other cell lines, including TSC2$^{-/-}$ EEF8 cells (fibroblast) and TSC1$^{-/-}$ MEF cells. We observed that glucose deprivation induced apoptosis in both TSC2$^{-/-}$ EEF8 (Figures 7E and 7F) and TSC1$^{-/-}$ MEF cells (Figures 7G and 7H). These results indicate that both TSC1 and TSC2 play an essential role in cellular energy response.

Cell Size Regulation by ATP Depletion and TSC2

TSC2 has been demonstrated to play a critical role in cell size control in *Drosophila*. We observed that the knockdown of TSC2 by RNAi resulted in a reproducible increase in HEK293 cell size even though the effect is small (Figure 8A). The small effect of RNAi on cell size could be due to an incomplete elimination of TSC2 by RNAi. We found that 2DG treatment significantly decreased cell size (Figure 8A). Knockdown of TSC2 by RNAi partially blocked the cell size decrease induced by 2DG. The cell size effects of TSC2 RNAi and 2DG are cell cycle independent as these treatments similarly affect both G1 and G2 cells. These results demonstrate

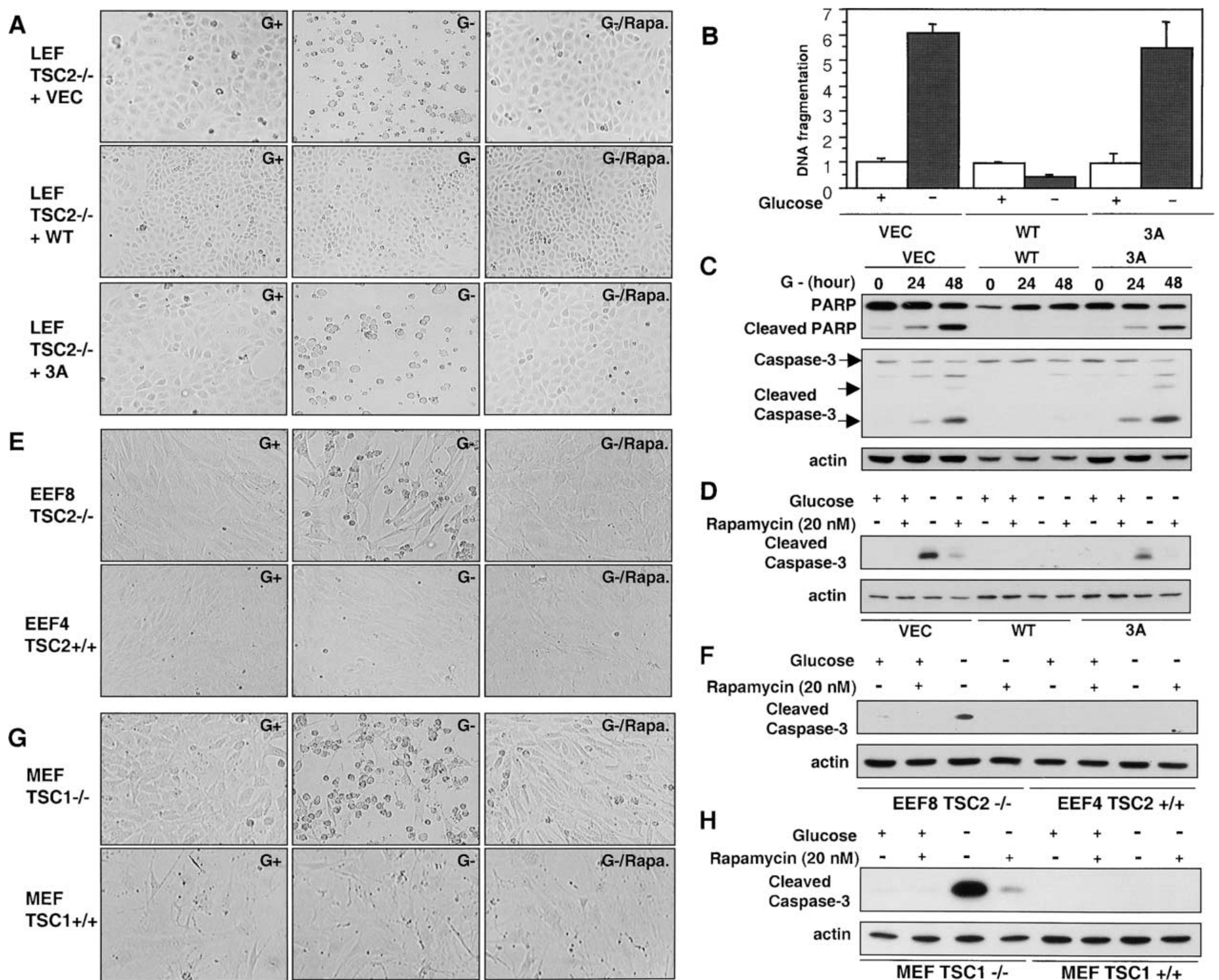

Figure 7. TSC2 Plays Essential Roles in Protecting Cells from Glucose Depletion-Induced Apoptosis

(A) TSC2 and rapamycin, but not TSC2-3A, protect LEF cells from glucose depletion-induced cell death. LEF cells stably expressing vector, TSC2, or TSC2-3A were cultured in 25 mM glucose (G+) or glucose-free medium (G-) with or without 20 nM rapamycin. Pictures were taken at 72 hr in culture. Note that the TSC2 wild-type expressing cells are morphologically smaller.

(B) Glucose depletion induces DNA fragmentation in vector and TSC2-3A but not in TSC2-expressing LEF cells. Cells were cultured in glucose-free medium for 48 hr. Both floating and attaching cells were harvested and histone-associated DNA fragmentation was measured.

(C) Glucose depletion induces cleavage of caspase-3 and PARP in vector and TSC2-3A but not in TSC2-expressing LEF cells. Western blot with caspase-3 and PARP antibody was performed.

(D) Rapamycin inhibits glucose depletion-induced caspase-3 activation in LEF cells. LEF cells stably expressing vector, TSC2, or TSC2-3A were cultured in glucose-free medium with or without 20 nM rapamycin for 48 hr. Western blots with anticleaved-caspase-3 and actin were shown.

(E) Effect of glucose depletion on cell death in EEF8 ($TSC2^{-/-}$) and EEF4 ($TSC2^{+/+}$) cells. EEF cells were cultured in glucose-free medium with or without 20 nM rapamycin for 96 hr.

(F) Effect of glucose depletion on caspase-3 activation in EEF cells. The EEF4 and EEF8 cells were cultured in glucose-free medium with or without 20 nM rapamycin for 72 hr. Western blots with cleaved-caspase-3 and actin were shown.

(G) Effect of glucose depletion on cell death in MEF ($TSC1^{+/+}$) and MEF ($TSC1^{-/-}$) cells. The MEFs were cultured in glucose-free medium for 48 hr.

(H) Effect of glucose depletion on caspase-3 activation in MEF ($TSC1^{+/+}$) and MEF ($TSC1^{-/-}$) cells. MEFs were cultured in glucose-free medium with or without 20 nM rapamycin for 16 hr. Experiments were same as Figure 7F.

that TSC2 plays an important role in 2DG-induced cell size reduction.

The effect of glucose starvation on cell size was also investigated. HEK293 cells cultured in 2.8 mM glucose (normal medium has 25 mM glucose) for 72 hr showed a significant reduction of cell size (Figure 8B). This result, together with the 2DG experiment described above, demonstrates that cellular energy starvation decreases cell size. Treatment with rapamycin also decreased cell size as previously reported (Figures 8A and 8B) (Fingar et al., 2002). These data are consistent with that TSC2 mediates the energy limitation signal to regulate cell size.

We observed that TSC2-expressing LEF cells are significantly smaller than the vector- or TSC2-3A-expressing cells (Figure 7A). FACS analysis studies confirmed that expression of TSC2 decreased the size of LEF $TSC2^{-/-}$ cells (Figure 8C). Interestingly, TSC2-3A showed

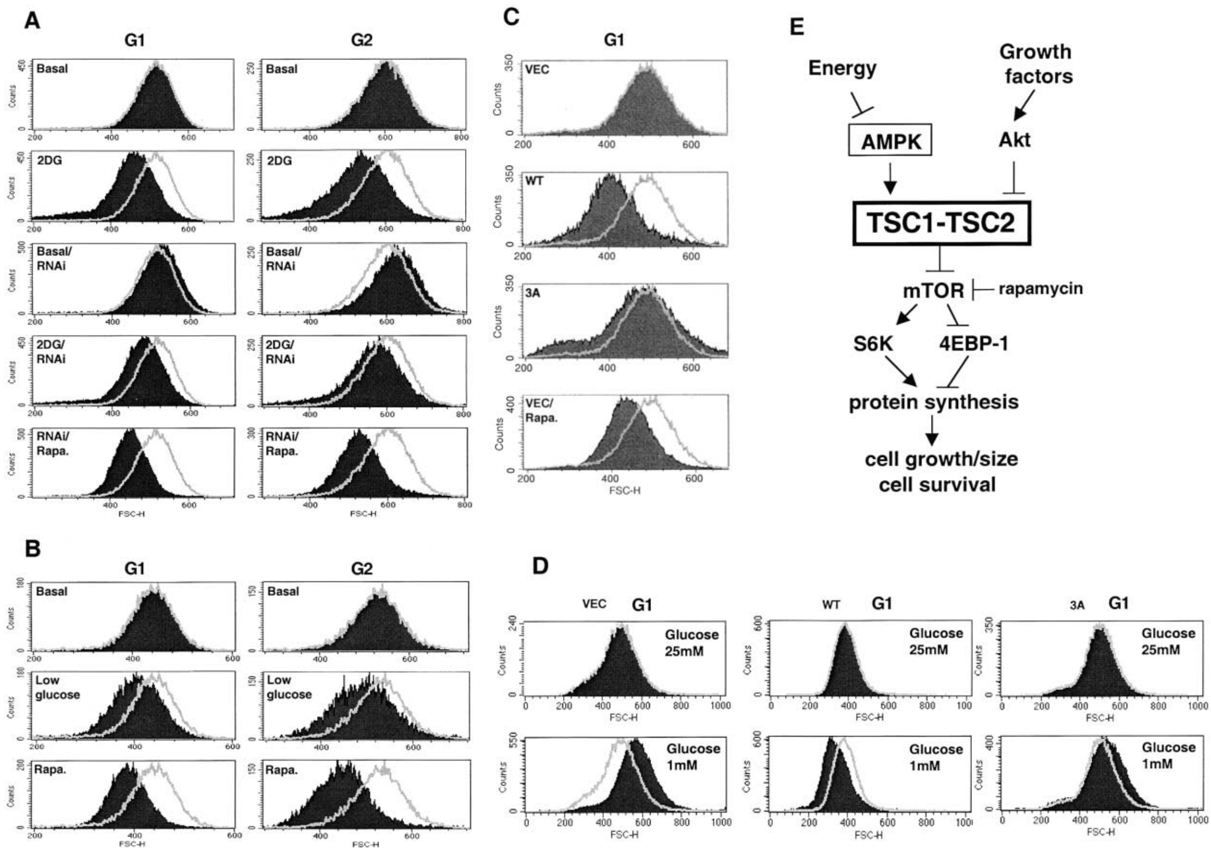

Figure 8. TSC2 Plays Critical Roles for Cell Size Control in Response to Energy Starvation

(A) 2DG decreases cell size in HEK293 cells. HEK293 cells were cultured in the presence of 12.5 mM 2DG, TSC2 RNAi, or 20 nM rapamycin for 72 hr. Cells were harvested and FACS analysis was performed to determine cell size. The X-axis indicates relative cell size. Cell size distribution curve of the control, as indicated by the gray curve, is included in each image for comparison purpose.

(B) Low glucose (2.8 mM) decreases cell size in HEK293 cells. Experiments are similar to those in (A).

(C) TSC2-3A is defective in cell size regulation. LEF cells stably expressing TSC2, TSC2-3A, and vector control were subjected to FACS analysis for cell size determination.

(D) The AMPK dependent phosphorylation of TSC2 is required for the function of TSC2 in cell size regulation by energy starvation. The TSC2$^{-/-}$ LEF cells stably expressing TSC2, TSC2-3A, and vector were cultured in 25 mM (upper images) or 1 mM glucose (lower images) containing media for 96 hr as indicated. Cells were harvested and FACS analysis was performed. Cell size distributions of G1 population are shown.

(E) A proposed model of TSC2 in cellular energy-signaling pathway. TSC2 receives signals from AMPK, which directly sensing cellular AMP/ATP ratio, to inhibit mTOR signaling. This model predicts that TSC1/TSC2 plays an important physiological function to control protein synthesis, cell size, and cell viability in response to cellular energy levels.

a lessened ability to reduce cell size in the LEF TSC2$^{-/-}$ cells when compared to wild-type TSC2, supporting that AMPK phosphorylation increases TSC2 function.

To demonstrate the physiological relevance of AMPK phosphorylation of TSC2 in cell size control, we examined the effect of glucose limitation on cell size. We tested various concentrations of glucose and found that 1 mM glucose is the lowest concentration that does not induce significant apoptosis in the TSC2$^{-/-}$ LEF cells. FACS analyses showed that 1 mM glucose did not reduce cell size of the TSC2$^{-/-}$ LEF cells (Figure 8D). Interestingly, 1 mM glucose significantly increased cell size of the TSC2$^{-/-}$ cells. These observations demonstrate that TSC2 plays an important role in cell size control in response to energy starvation. The TSC2- and TSC2-3A-expressing cells were also cultured in 1 mM glucose. As expected, expression of wild-type TSC2 restored the normal cellular energy response, a significant cell size reduction by energy starvation (Figure 8D). In contrast, the TSC2-3A-expressing cells did not restore normal cellular energy response and behaved indistinguishably from the TSC2$^{-/-}$ cells. Energy starvation caused a significant cell size increase of the TSC2-3A-expressing cells (Figure 8D). The above data demonstrate that the AMPK dependent phosphorylation plays an essential role for the physiological functions of TSC2 to regulate cell size in response to cellular energy starvation. A possible explanation for the cell size increase in the TSC2$^{-/-}$ cells is that the TSC2$^{-/-}$ cells are unable to respond to energy starvation and continue to grow despite of the low energy levels. However, energy limitation may prevent cell cycle progression by activating cell cycle checkpoints. Therefore, the TSC2$^{-/-}$ and the TSC2-3A-expressing cells are increased in cell size under low glucose conditions but will die under glucose-free conditions. These observations are completely con-

sistent with our model that TSC2 plays an essential role in the coordination between cell growth and cellular energy levels.

Discussion

The coordination between cell growth and cellular energy levels is a fundamental question in cell biology and has not been fully understood. This study provides a molecular mechanism how cellular energy starvation activates TSC2, which then inhibits cell growth and enhances cell survival by inhibiting translation (Figure 8E). Therefore, TSC2 is an essential player in the coordination of cellular energy levels and cell growth or survival. Our model predicts that AMPK is a cellular energy sensor and activates TSC2 by direct phosphorylation. mTOR is a key downstream target of TSC2 to mediate the cellular response (Figure 8E).

Protein synthesis is a major cellular process regulated by a wide array of intracellular and extracellular conditions such as mitogenic growth factors, amino acid concentrations, and cellular energy levels. Protein synthesis utilizes approximately 20%–25% of the total cellular energy and must be tightly coordinated with cellular energy status (Schmidt, 1999). Inhibition of translation is a major physiological response under energy starvation conditions to maintain homeostasis. One of the major translation controls is mediated by the phosphorylation of S6K and 4EBP1 by mTOR (Proud, 2002). In this study, we demonstrated that TSC2 plays an important physiological role to inhibit mTOR signaling in response to cellular energy levels (Figure 7G). Phosphorylation of TSC2 by AMPK stimulates TSC2 activity to inhibit S6K and 4EBP1 phosphorylation. In contrast, phosphorylation of TSC2 by Akt relays the growth factor signals and suppresses the activity of TSC2. Our results demonstrate that the AMPK-dependent phosphorylation of TSC2 is required for ATP depletion-induced dephosphorylation of S6K and 4EBP1.

Based on our model, mTOR is in the energy-sensing pathway downstream of TSC1/TSC2 (Figure 8E). However, AMPK is likely the cellular energy sensor under most physiological and pathological conditions and functions upstream of TSC1/TSC2. Under extreme energy starvation conditions, mTOR may also function as a cellular energy sensor. AMPK can inhibit translation by at least two mechanisms, one by phosphorylation of the eukaryotic elongation factor 2 (eEF2) (Horman et al., 2002) and the other by phosphorylation of TSC2. We propose that activation of AMPK plays a major role in the inhibition of protein synthesis by suppressing the functions of multiple translation regulators including S6K, 4EBP1, and eEF2 in response to energy starvation and low metabolic conditions. Glucose deprivation induces massive apoptosis in TSC2$^{-/-}$ cells. Expression of wild-type TSC2 completely blocks apoptosis while expression of the TSC2-3A mutant fails to protect cells from apoptosis. Similarly, glucose starvation also induces apoptosis in TSC1$^{-/-}$ cells. Furthermore, mTOR is a key downstream target of TSC1/TSC2 because inhibition of mTOR by rapamycin significantly suppressed energy starvation-induced apoptosis in TSC2$^{-/-}$ and TSC1$^{-/-}$ cells. These observations demonstrate that the TSC-mTOR pathway plays a major role in regulation of cell survival under energy starvation conditions.

The function of TSC2 in the cellular energy response is further supported by the fact that energy limitation by glucose deprivation or 2DG treatment decreases cell size. Consistently, TSC2 expression also reduces cell size. Therefore, energy limitation and TSC2 have similar effects on cell size control. The energy starvation-induced cell size reduction is abolished in TSC2$^{-/-}$ cells. Expression of wild-type, but not the AMPK phosphorylation mutant TSC2, restores the energy starvation-induced cell size reduction. These observations clearly established the physiological importance of AMPK phosphorylation of TSC2 in cellular energy response. It is conceivable that the activation of TSC2 by AMPK-dependent phosphorylation results in a decrease of protein synthesis and conservation of cellular energy (Figure 8E). Consistent with this model, rapamycin significantly protects LEF cells from glucose deprivation-induced apoptosis. The inability of TSC2$^{-/-}$ cells to suppress translation initiation under the energy starvation condition could produce the detrimental effects and trigger apoptosis.

The identification of TSC2 as an important physiological substrate of AMPK may provide a mechanism of AMPK mutation in human disease. AMPKγ subunits mutations have been implicated in familial hypertrophic cardiomyopathy (Hardie and Hawley, 2001). TSC2 homozygous mutation shows a lethal phenotype with cardiac hypertrophy. Furthermore, inhibition of mTOR by rapamycin has been documented in the suppression of cardiac hypertrophy (Shioi et al., 2003). TSC2 is a prominent negative regulator of cell size control in *Drosophila* (Potter and Xu, 2001) and in mammalian cells from this study. All these observations are consistent with our model that TSC2 acts downstream of AMPK to inhibit mTOR. This may suggest a possible mechanistic role of TSC2 in mediating the function of AMPK in cardiac hypertrophy.

LKB1 is a tumor suppressor gene and mutation of LKB1 is responsible for the Peutz-Jeghers syndrome (Hemminki et al., 1998; Jenne et al., 1998). The molecular mechanism for LKB1 as a tumor suppressor has been unclear because key physiological substrates of LKB1 were previously unknown. It has been recently demonstrated that LKB1 is the upstream activating kinase for AMPK (Hong et al., 2003; Sutherland et al., 2003; Hawley et al., 2003). LKB1 directly phosphorylates AMPK in the activation loop and increases AMPK kinase activity. Peutz-Jeghers syndrome is characterized by multiple hamartomas mainly in the intestine. Interestingly, the hamartomas in Peutz-Jeghers syndrome are similar to the benign tumors seen in TSC, although the tumors develop in different tissues (Yoo et al., 2002). These observations taken together with our findings described in this paper suggest one possible molecular mechanism for the tumor suppressor functions of LKB1, where the LKB1 tumor suppressor may activate the TSC2 tumor suppressor via the AMPK.

In conclusion, our data demonstrate that TSC2 plays an important role in the coordination between cellular energy levels, and cell growth and survival. TSC2 integrates signals from multiple pathways to regulate translation, cell size, and apoptosis. Activation of TSC2 by

AMPK-dependent phosphorylation prepares cells for an unfavorable growth environment and results in protection from cell death. In addition to causing tuberous sclerosis, inactivation of the TSC1/TSC2 tumor suppressor complex could be a key event in oncogenic pathways and cellular hypertrophy.

Experimental Procedures

Materials

Anti-TSC2 (C-20) was from Santa Cruz Biotechnology. Anti-TSC1 antibody was generously provided by Dr. Y. Xiong (University of North Carolina). All another antibodies were from Cell Signaling. Human TSC1 (Myc-TSC1), rat TSC2 (HA-TSC2), and rat S6K1-α II (HA-S6K) constructs were described previously (Inoki et al., 2002). The cDNAs encoding human AMPK αI and α II subunit were obtained by PCR and subcloned into pcDNA3-HA vector. To generate GST-fusion of TSC2, TSC2 fragments were expressed in pGEX-KG vector. All mutant constructs of TSC2, GST-fusion TSC2 fragments, AMPK (AMPK αI D159A, AMPK αI aa.1-314 T174D, AMPK αII D157A, and AMPK αII aa.1-313 T172D) were created by PCR mutagenesis and were verified by DNA sequencing. Compound C (AMPK inhibitor) was obtained from MERCK.

Cell Culture, Stimulation, Transfection, and Retrovirus Infection

HEK293 cells, TSC1$^{-/-}$, and TSC1$^{+/+}$ MEF cells were cultured in Dulbecco's modified Eagle's medium (DMEM) (Invitrogen) containing 10% fetal bovine serum (FBS) (Invitrogen). For ATP depletion, the cells were stimulated by 2DG and various other ATP-depletion reagents. One hour prior to stimulation, the culture media were replaced with serum-free DMEM containing 25 mM D-glucose. The cells were then stimulated by the 10× 2DG solutions in DMEM for indicated time. For glucose starvation, the cells were cultured with D-glucose-free DMEM containing 25 mM HEPES and 10% dialyzed FBS. Transfections were performed in serum-free condition using lipofectamine reagent (Invitrogen). EEF126-4 (EEF4, TSC2$^{+/+}$), EEF126-8 (EEF8, TSC2$^{-/-}$) and LExF2 (LEF) (TSC2$^{-/-}$) cells were cultured in DMEM/F12 (Invitrogen) containing 10% FBS. The wild-type or mutant rat TSC2 cDNA was subcloned into the retroviral vector pPGS-CMV-CITE-Neo. The Phoenix retrovirus packaging cells were transfected with the empty retrovirus vectors or the vector containing TSC2 or TSC2 mutants using lipofectamine reagent (Invitrogen). Forty hr after transfection, the retrovirus generated by the Phoenix cells was used for infection of EEF8 and LEF.

Nucleotides Measurement and Statistical Analysis

HEK 293 cells cultured in a 12-well dish were treated with the indicated concentrations of 2DG for 15 min. The cells were scraped into the buffer (100 mM Tris-HCl [pH 7.75], 4 mM EDTA) and immediately frozen in liquid nitrogen. The frozen cells were lysed by boiling for 5 min and then placed on ice for 5 min before the ATP levels in the supernatants were measured using a luciferase-based assay (ATP Bioluminescence Assay Kit CLS II, Roche). To determine the ratio of AMP/ATP, the cellular concentrations of AMP and ATP were measured by high-pressure liquid chromatography (HPLC). For statistical analysis, differences between groups were assessed by ANOVA or Student's t-test followed by Bonferroni's post hoc comparison between selected groups.

RNA Interference

TSC2 RNAi experiments were performed as published (Inoki et al., 2002).

Metabolic Labeling and Two-Dimensional Phosphopeptide Mapping

Metabolic labeling and peptide mapping were performed as before (Inoki et al., 2002) except for using different chromatography buffer (n-butanol/pyridine/acetic acid/water, 75:50:24:50).

Immunoprecipitations and Kinase Assay

Cells were lysed in lysis buffer N (10 mM Tris-HCl [pH 7.5], 100 mM NaCl, 1% NP-40, 50 mM NaF, 2 mM EDTA, 1 mM DTT, 1 mM PMSF, 10 μg/ml leupeptin, and 10 μg/ml aprotinin) and immunoprecipitated with HA antibody and protein G-Sepharose beads (Amersham Biosciences). Immunocomplexes were subjected to SDS-PAGE. To study the interaction between TSC2 and AMPK, HEK 293 cells were harvested in the buffer I (20 mM Tris-HCl [pH 7.5], 20 mM NaCl, 1 mM EDTA, 5 mM EGTA, 20 mM β-glycerophosphate, 1 mM DTT, 1 mM PMSF, 10 μg/ml leupeptin, and 10 μg/ml aprotinin) and sonicated. The cell lysates were immunoprecipitated with the indicated antibodies and immobilized protein A (PIERCE). Immunocomplexes were washed twice with buffer I containing 0.5 M NaCl and then washed twice with buffer II (10 mM HEPES [pH 7.4], 50 mM NaCl, 20 mM β-glycerophosphate, and 20 mM NaF) and then subjected to SDS-PAGE.

For the AMPK kinase assays, HEK293 cells were transfected with AMPK αI or AMPK αI D159A (kinase inactive) constructs. Transfected HEK 293 cells were treated with 50 mM 2DG for 30 min and then lysed in lysis buffer A (50 mM Tris-HCl [pH 7.5], 50 mM NaF, 5 mM pyrophosphate, 1 mM EDTA, 1 mM DTT, 10% glycerol, 1% Triton X-100, 1 mM PMSF, 10 μg/ml leupeptin, and 10 μg/ml aprotinin) and immunoprecipitated by HA antibody and protein G-Sepharose beads. The immunoprecipitates were washed twice with buffer A and then washed twice with buffer B (50 mM HEPES [pH 7.5], 1 mM EDTA, 1 mM DTT, 10% glycerol) and once with buffer N and once with HEPES buffer (25 mM HEPES [pH 8], 0.5 mM EDTA, 0.025% β-mercaptoethanol). Immunoprecipitated AMPK and AMPK kinase inactive were subjected to a kinase assay using purified bacterial-derived TSC2 fragments as substrates.

Cell Size and Cell Viability Assay

To determine cell size and DNA content, FACS analysis with Cell Quest software was performed. For HEK293 cell size experiments, confluent cells in 10 cm dish were replated to 10 cm dish (1:10–20 split). After 16 hr, the cells were cultured under indicated conditions for 72 hr. The cultured medium was changed every 24 hr. To harvest cells, plates were washed once phosphate saline buffer (PBS) and incubated at 37°C for 2 min in 2 ml trypsin-EDTA. Cells were gently pipetted off the plate with PBS/10% FBS, transferred to 15 ml conical tubes, centrifuged for 3 min at 1000 rpm, once washed with PBS/1% FBS, and the final cells pellets were resuspended with 1 ml of PBS/1% FBS. Resuspended cells were fixed on ice by adding cold 3 ml of 100% ethanol (75% final). Fixed cells were stored at 4°C until the time of analysis. Immediately before analysis on FACS, the fixed cells were centrifuged at 1500 rpm for 3 min washed once with PBS/1% FBS, and then incubated at 37°C for 20 min in 1 ml of PBS/1% FBS containing 0.1% Triton X-100 and 250 μg/ml RNAase A. The cells were stained by propidium iodide for FACS analysis to determine the cells size in G1-phase and G2-phase populations. For LEF cells size analysis, completely trypsinized cells were seeded to 10 cm dish at 20% confluency and then cultured with DMEM/F12 5% FBS in the presence or absence of 20 nM rapamycin for indicated hours. The cells were analyzed by FACS as described above.

For DNA fragment assay, LEF cells were cultured with DMEM/10% dialyzed FBS in the presence or absence of 25 mM D-glucose for 48 hr. To detect apoptotic cell death, the mono- and oligonucleosomes in cytoplasmatic fraction of cell lysates were determined by ELISA using cell death detection ELISAplus Kit (Roche).

Acknowledgments

We are indebted to Dr. R.S. Yeung for providing EEF126 cell lines and the LExF2 cell line; Dr. D.J. Kwiatkowski for TSC1$^{-/-}$, $^{+/+}$ MEFs; Dr. G. Zhou for the AMPK inhibitor; and Dr. J.M. Weinberg for assistance in determination of AMP and ATP. We thank Drs. H.G. Vikis, K. Stankunas, and Y. Li for comments and suggestions. We also thank H. Chong, J. Aurandt for critical reading of the manuscript. This work was supported by grants from the National Institutes of Health and the Walther Cancer Institute.

Received: April 9, 2003
Revised: October 7, 2003
Accepted: November 7, 2003
Published: November 25, 2003

References

Au, K.S., Rodriguez, J.A., Finch, J.L., Volcik, K.A., Roach, E.S., Delgado, M.R., Rodriguez, E., Jr., and Northrup, H. (1998). Germ-line mutational analysis of the TSC2 gene in 90 tuberous-sclerosis patients. Am. J. Hum. Genet. *62*, 286–294.

Brown, E.J., Beal, P.A., Keith, C.T., Chen, J., Shin, T.B., and Schreiber, S.L. (1995). Control of p70 s6 kinase by kinase activity of FRAP in vivo. Nature *377*, 441–446.

Browne, G.J., and Proud, C.G. (2002). Regulation of peptide-chain elongation in mammalian cells. Eur. J. Biochem. *269*, 5360–5368.

Corton, J.M., Gillespie, J.G., Hawley, S.A., and Hardie, D.G. (1995). 5-aminoimidazole-4-carboxamide ribonucleoside. A specific method for activating AMP-activated protein kinase in intact cells? Eur. J. Biochem. *229*, 558–565.

Dan, H.C., Sun, M., Yang, L., Feldman, R.I., Sui, X.M., Yeung, R.S., Halley, D.J., Nicosia, S.V., Pledger, W.J., and Cheng, J.Q. (2002). PI3K/AKT pathway regulates TSC tumor suppressor complex by phosphorylation of tuberin. J. Biol. Chem. *277*, 35364–35370.

Dennis, P.B., Jaeschke, A., Saitoh, M., Fowler, B., Kozma, S.C., and Thomas, G. (2001). Mammalian TOR: a homeostatic ATP sensor. Science *294*, 1102–1105.

Fingar, D.C., Salama, S., Tsou, C., Harlow, E., and Blenis, J. (2002). Mammalian cell size is controlled by mTOR and its downstream targets S6K1 and 4EBP1/eIF4E. Genes Dev. *16*, 1472–1487.

Gao, X., and Pan, D. (2001). TSC1 and TSC2 tumor suppressors antagonize insulin signaling in cell growth. Genes Dev. *15*, 1383–1392.

Gao, X., Zhang, Y., Arrazola, P., Hino, O., Kobayashi, T., Yeung, R.S., Ru, B., and Pan, D. (2002). Tsc tumour suppressor proteins antagonize amino-acid-TOR signalling. Nat. Cell Biol. *4*, 699–704.

Goncharova, E.A., Goncharov, D.A., Eszterhas, A., Hunter, D.S., Glassberg, M.K., Yeung, R.S., Walker, C.L., Noonan, D., Kwiatkowski, D.J., Chou, M.M., et al. (2002). Tuberin Regulates p70 S6 Kinase Activation and Ribosomal Protein S6 Phosphorylation. A role for the Tsc2 tumor suppressor gene in pulmonary lymphangeioleiomyomatosis (LAM). J. Biol. Chem. *277*, 30958–30967.

Hara, K., Yonezawa, K., Weng, Q.P., Kozlowski, M.T., Belham, C., and Avruch, J. (1998). Amino acid sufficiency and mTOR regulate p70 S6 kinase and eIF-4E BP1 through a common effector mechanism. J. Biol. Chem. *273*, 14484–14494.

Hardie, D.G., and Hawley, S.A. (2001). AMP-activated protein kinase: the energy charge hypothesis revisited. Bioessays *23*, 1112–1119.

Hardie, D.G., Carling, D., and Carlson, M. (1998). The AMP-activated/SNF1 protein kinase subfamily: metabolic sensors of the eukaryotic cell? Annu. Rev. Biochem. *67*, 821–855.

Hawley, S.A., Boudeau, J., Reid, J.L., Mustard, K.J., Udd, L., Makela, T.P., Alessi, D.R., and Hardie, D.G. (2003). Complexes between the LKB1 tumor suppressor, STRADalpha/beta and MO25alpha/beta are upstream kinases in the AMP-activated protein kinase cascade. J. Biol. *2*, 28.

Hemminki, A., Markie, D., Tomlinson, I., Avizienyte, E., Roth, S., Loukola, A., Bignell, G., Warren, W., Aminoff, M., Hoglund, P., et al. (1998). A serine/threonine kinase gene defective in Peutz-Jeghers syndrome. Nature *391*, 184–187.

Hong, S.P., Leiper, F.C., Woods, A., Carling, D., and Carlson, M. (2003). Activation of yeast Snf1 and mammalian AMP-activated protein kinase by upstream kinases. Proc. Natl. Acad. Sci. USA *100*, 8839–8843.

Horman, S., Browne, G., Krause, U., Patel, J., Vertommen, D., Bertrand, L., Lavoinne, A., Hue, L., Proud, C., and Rider, M. (2002). Activation of AMP-activated protein kinase leads to the phosphorylation of elongation factor 2 and an inhibition of protein synthesis. Curr. Biol. *12*, 1419–1423.

Inoki, K., Li, Y., Zhu, T., Wu, J., and Guan, K.L. (2002). TSC2 is phosphorylated and inhibited by Akt and suppresses mTOR signalling. Nat. Cell Biol. *4*, 648–657.

Ito, N., and Rubin, G.M. (1999). gigas, a Drosophila homolog of tuberous sclerosis gene product-2, regulates the cell cycle. Cell *96*, 529–539.

Jaeschke, A., Hartkamp, J., Saitoh, M., Roworth, W., Nobukuni, T., Hodges, A., Sampson, J., Thomas, G., and Lamb, R. (2002). Tuberous sclerosis complex tumor suppressor-mediated S6 kinase inhibition by phosphatidylinositide-3-OH kinase is mTOR independent. J. Cell Biol. *159*, 217–224.

Jenne, D.E., Reimann, H., Nezu, J., Friedel, W., Loff, S., Jeschke, R., Muller, O., Back, W., and Zimmer, M. (1998). Peutz-Jeghers syndrome is caused by mutations in a novel serine threonine kinase. Nat. Genet. *18*, 38–43.

Kenerson, H.L., Aicher, L.D., True, L.D., and Yeung, R.S. (2002). Activated mammalian target of rapamycin pathway in the pathogenesis of tuberous sclerosis complex renal tumors. Cancer Res. *62*, 5645–5650.

Kimura, N., Tokunaga, C., Dalal, S., Richardson, C., Yoshino, K., Hara, K., Kemp, B.E., Witters, L.A., Mimura, O., and Yonezawa, K. (2003). A possible linkage between AMP-activated protein kinase (AMPK) and mammalian target of rapamycin (mTOR) signalling pathway. Genes Cells *8*, 65–79.

Kobayashi, T., Minowa, O., Sugitani, Y., Takai, S., Mitani, H., Kobayashi, E., Noda, T., and Hino, O. (2001). A germ-line Tsc1 mutation causes tumor development and embryonic lethality that are similar, but not identical to, those caused by Tsc2 mutation in mice. Proc. Natl. Acad. Sci. USA *98*, 8762–8767.

Krause, U., Bertrand, L., and Hue, L. (2002). Control of p70 ribosomal protein S6 kinase and acetyl-CoA carboxylase by AMP-activated protein kinase and protein phosphatases in isolated hepatocytes. Eur. J. Biochem. *269*, 3751–3759.

Kwiatkowski, D.J. (2003). Tuberous sclerosis: from tubers to mTOR. Ann. Hum. Genet. *67*, 87–96.

Kwiatkowski, D.J., Zhang, H., Bandura, J.L., Heiberger, K.M., Glogauer, M., el-Hashemite, N., and Onda, H. (2002). A mouse model of TSC1 reveals sex-dependent lethality from liver hemangiomas, and up-regulation of p70S6 kinase activity in Tsc1 null cells. Hum. Mol. Genet. *11*, 525–534.

Manning, B.D., Tee, A.R., Logsdon, M.N., Blenis, J., and Cantley, L.C. (2002). Identification of the tuberous sclerosis complex-2 tumor suppressor gene product tuberin as a target of the phosphoinositide 3-kinase/akt pathway. Mol. Cell *10*, 151–162.

Nave, B.T., Ouwens, M., Withers, D.J., Alessi, D.R., and Shepherd, P.R. (1999). Mammalian target of rapamycin is a direct target for protein kinase B: identification of a convergence point for opposing effects of insulin and amino-acid deficiency on protein translation. Biochem. J. *344*, 427–431.

Onda, H., Lueck, A., Marks, P.W., Warren, H.B., and Kwiatkowski, D.J. (1999). Tsc2(+/−) mice develop tumors in multiple sites that express gelsolin and are influenced by genetic background. J. Clin. Invest. *104*, 687–695.

Onda, H., Crino, P.B., Zhang, H., Murphey, R.D., Rastelli, L., Gould Rothberg, B.E., and Kwiatkowski, D.J. (2002). Tsc2 null murine neuroepithelial cells are a model for human tuber giant cells, and show activation of an mTOR pathway. Mol. Cell. Neurosci. *21*, 561–574.

Potter, C.J., and Xu, T. (2001). Mechanisms of size control. Curr. Opin. Genet. Dev. *11*, 279–286.

Potter, C.J., Huang, H., and Xu, T. (2001). Drosophila Tsc1 functions with Tsc2 to antagonize insulin signaling in regulating cell growth, cell proliferation, and organ size. Cell *105*, 357–368.

Potter, C.J., Pedraza, L.G., and Xu, T. (2002) Akt regulates growth by directly phosphorylating TSC2. Nat. Cell. Biol. *4*, 659–665.

Proud, C.G. (2002). Regulation of mammalian translation factors by nutrients. Eur. J. Biochem. *269*, 5338–5349.

Radimerski, T., Montagne, J., Hemmings-Mieszczak, M., and Thomas, G. (2002). Lethality of Drosophila lacking TSC tumor sup-

pressor function rescued by reducing dS6K signaling. Genes Dev. *16*, 2627–2632.

Schmidt, E.V. (1999). The role of c-myc in cellular growth control. Oncogene *18*, 2988–2996.

Scott, P.H., Brunn, G.J., Kohn, A.D., Roth, R.A., and Lawrence, J.C., Jr. (1998). Evidence of insulin-stimulated phosphorylation and activation of the mammalian target of rapamycin mediated by a protein kinase B signaling pathway. Proc. Natl. Acad. Sci. USA *95*, 7772–7777.

Scott, J.W., Norman, D.G., Hawley, S.A., Kontogiannis, L., and Hardie, D.G. (2002). Protein kinase substrate recognition studied using the recombinant catalytic domain of AMP-activated protein kinase and a model substrate. J. Mol. Biol. *317*, 309–323.

Sekulic, A., Hudson, C.C., Homme, J.L., Yin, P., Otterness, D.M., Karnitz, L.M., and Abraham, R.T. (2000). A direct linkage between the phosphoinositide 3-kinase-AKT signaling pathway and the mammalian target of rapamycin in mitogen-stimulated and transformed cells. Cancer Res. *60*, 3504–3513.

Shah, O.J., Anthony, J.C., Kimball, S.R., and Jefferson, L.S. (2000). 4E–BP1 and S6K1: translational integration sites for nutritional and hormonal information in muscle. Am. J. Physiol. Endocrinol. Metab. *279*, E715–E729.

Shioi, T., McMullen, J.R., Tarnavski, O., Converso, K., Sherwood, M.C., Manning, W.J., and Izumo, S. (2003). Rapamycin attenuates load-induced cardiac hypertrophy in mice. Circulation *107*, 1664–1670.

Soltoff, S.P. (2001). Rottlerin is a mitochondrial uncoupler that decreases cellular ATP levels and indirectly blocks protein kinase Cdelta tyrosine phosphorylation. J. Biol. Chem. *276*, 37986–37992.

Stein, S.C., Woods, A., Jones, N.A., Davison, M.D., and Carling, D. (2000). The regulation of AMP-activated protein kinase by phosphorylation. Biochem. J. *345*, 437–443.

Sutherland, C.M., Hawley, S.A., McCartney, R.R., Leech, A., Stark, M.J., Schmidt, M.C., and Hardie, D.G. (2003). Elm1p is one of three upstream kinases for the Saccharomyces cerevisiae SNF1 complex. Curr. Biol. *13*, 1299–1305.

Tapon, N., Ito, N., Dickson, B.J., Treisman, J.E., and Hariharan, I.K. (2001). The Drosophila tuberous sclerosis complex gene homologs restrict cell growth and cell proliferation. Cell *105*, 345–355.

Tee, A.R., Fingar, D.C., Manning, B.D., Kwiatkowski, D.J., Cantley, L.C., and Blenis, J. (2002). Tuberous sclerosis complex-1 and -2 gene products function together to inhibit mammalian target of rapamycin (mTOR)-mediated downstream signaling. Proc. Natl. Acad. Sci. USA *99*, 13571–13576.

van Slegtenhorst, M., Nellist, M., Nagelkerken, B., Cheadle, J., Snell, R., van den Ouweland, A., Reuser, A., Sampson, J., Halley, D., and van der Sluijs, P. (1998). Interaction between hamartin and tuberin, the TSC1 and TSC2 gene products. Hum. Mol. Genet. *7*, 1053–1057.

Yoo, L.I., Chung, D.C., and Yuan, J. (2002). LKB1–a master tumour suppressor of the small intestine and beyond. Nat. Rev. Cancer *2*, 529–535.

Young, J., and Povey, S. (1998). The genetic basis of tuberous sclerosis. Mol. Med. Today *4*, 313–319.

Zhou, G., Myers, R., Li, Y., Chen, Y., Shen, X., Fenyk-Melody, J., Wu, M., Ventre, J., Doebber, T., Fujii, N., et al. (2001). Role of AMP-activated protein kinase in mechanism of metformin action. J. Clin. Invest. *108*, 1167–1174.